



---

**EFFECT OF Li<sup>1+</sup> SUBSTITUTION ON ELASTIC PROPERTIES OF Ni-Zn FERRITES**

---

<sup>1</sup>N.D.Chaudhari, <sup>2</sup>P. V. Patil, <sup>1</sup>B. R. Sharma and <sup>1\*</sup>P. R. Kute

<sup>1</sup>Pratishthan Mahavidyalaya, Paithan, Dist. Aurangabad

<sup>2</sup>Vidya Pratishthan's Arts, Comm., Sci. College, Baramati

<sup>1\*</sup>Corresponding author email –kuteprabhakar@gmail.com

---

**ABSTRACT**

Li<sup>1+</sup> substituted Ni-Zn ferrites were synthesized using oxalate precursor method. FTIR spectra of synthesized compositions were recorded from 350 to 800 cm<sup>-1</sup>. Two absorption bands corresponding to tetrahedral and octahedral sites were observed between (579-591 cm<sup>-1</sup>) and (407-424 cm<sup>-1</sup>). The force constant for tetrahedral and octahedral sites were determined and found to decrease with increase in Li<sup>1+</sup> content. Elastic parameters such as Young's modulus, Bulk modulus, Modulus of rigidity, Debye temperature, Wave velocity were estimated as a function of composition and corrected to zero porosity. All these elastic moduli are observed to decrease with increasing Li<sup>1+</sup> concentration. The bulk modulus to rigidity modulus ratio indicates the brittle nature of synthesized material.

**KEYWORDS:** oxalate precursor method , tetrahedral and octahedral.

**INTRODUCTION:**

Soft ferrites have attracted a lot of attention due to their technological applications. Ni-Zn ferrites are the versatile magnetic material due to their high electrical resistivity, high saturation magnetization, low losses, moderate permeability, high mechanical hardness, more chemical stability and high Curie temperature [1-3]. Ni-Zn ferrites are mainly used in high frequency applications particularly at microwaves [3]. The fundamental properties of ferrite materials are very much sensitive to many parameters such as method of preparation, nature and amount of substitution and distribution of cations [4-6]. Many synthesis techniques such as ceramic [7], sol-gel [8], hydrothermal [9], co-precipitation [10], combustion route [11] have been used for the preparation of ferrite materials.

Ferrites synthesized using ceramic method involves high reaction temperature, long reaction time resulting in large particles with non-uniform in size. To overcome these difficulties the chemical routes have been considered and employed for the preparation of ferrite to get homogeneous product [8-11].

Many workers [12-15] have indicated that an introduction of relatively small amount of foreign ions in to Ni-Zn ferrites results in the modified electrical and magnetic properties. Study of elastic parameters of ferrite material is great importance to understand the behaviour of engineering materials and related to many physical properties of solids. They provide information about the nature of inter atomic and inter ionic binding forces in the materials [16-18]. The values of elastic parameters reveal high mechanical strength, fracture toughness and thermal shock tolerance. Therefore in the present study, it is decided to synthesize the various compositions of Li<sup>1+</sup> substituted Ni-Zn ferrites using oxalate precursor and study their elastic properties as a function of composition.

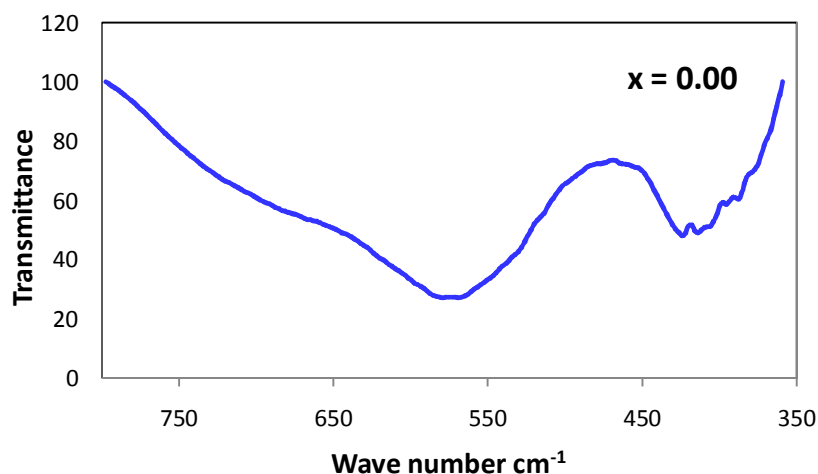
**EXPERIMENTAL:**

Various compositions of  $\text{Ni}_{0.32}\text{Zn}_{0.68-2x}\text{Li}_x\text{Fe}_{2-x}\text{O}_4$  ( $x = 0.00, 0.025, 0.05, 0.075, 0.10, 0.125, 0.150, 0.175$  and  $0.20$ ) have been synthesized using oxalate precursor method. Ni-Zn-Fe oxalates were synthesized using a method suggested by Wickham [19] and later on modified by M. Bremer et. al [20] for Mn-Zn ferrites. Lithium oxalates were prepared separately by the method suggested by Dollimore et. al [21]. The resulting all solid solution oxalates were mixed and decomposed at  $400^\circ\text{C}$  for three hours. The decomposed powder was again sintered at  $1050^\circ\text{C}$  for four hours in air atmosphere. These ferrite compositions thus prepared were characterized using FTIR to study effect of  $\text{Li}^{1+}$  substitution on vibrational bands and elastic properties of Ni-Zn ferrites. FTIR spectra were recorded in the range of  $350 - 800\text{ cm}^{-1}$  at room temperature.

**RESULT AND DISCUSSION:**

Fig. 1 (a, b, c) shows the FTIR spectra for  $\text{Ni}_{0.32}\text{Zn}_{0.68-2x}\text{Li}_x\text{Fe}_{2-x}\text{O}_4$  ferrites particles recorded at room temperature in the range of  $350 - 800\text{ cm}^{-1}$ . According to Waldron [22], ferrite material can be considered as continuously bonded crystal i.e the atoms are bonded to all the nearest neighbours by equivalent forces. In present the ferrite system, the appearance of two absorption bands corresponds to stretching vibration of tetrahedral and octahedral complexes ( $\nu_1$  and  $\nu_2$ ) confirms the formation of spinel type structure. The positions of  $\nu_1$  and  $\nu_2$  are tabulated in Table 1. It is observed that the absorption bands for present ferrite system are found to be in the expected range of high frequency band  $\nu_1$  is at  $579-591\text{ cm}^{-1}$  and low frequency band  $\nu_2$  is at  $407-426\text{ cm}^{-1}$ . Lavat and Baran [23, 24] suggested that the high frequency absorption peak in the range of  $600-500\text{ cm}^{-1}$  is assigned to intrinsic stretching vibration of bands between tetrahedral metal ion and oxygen ions and low frequency absorption peak to stretching vibration of bands between octahedral metal ion and oxygen ions. The positions of high frequency band  $\nu_1$  and low frequency band  $\nu_2$  slightly vary due to the difference in  $\text{Fe}^{3+}-\text{O}^{2-}$  distances for both tetrahedral and octahedral sites. The values of  $\nu_1$  are higher than the values of  $\nu_2$  indicates that the normal mode of vibration of tetrahedral complexes is higher than the corresponding octahedral sites. This behaviour may be attributed to the bond angles of tetrahedral and octahedral sites.

It is also observed that as  $\text{Li}^{1+}$  content increases in Ni-Zn ferrites  $\nu_1$  shifts to higher frequency side and  $\nu_2$  shift towards lower frequency side. This may be due to the changes in the cation distribution of spinel lattice.



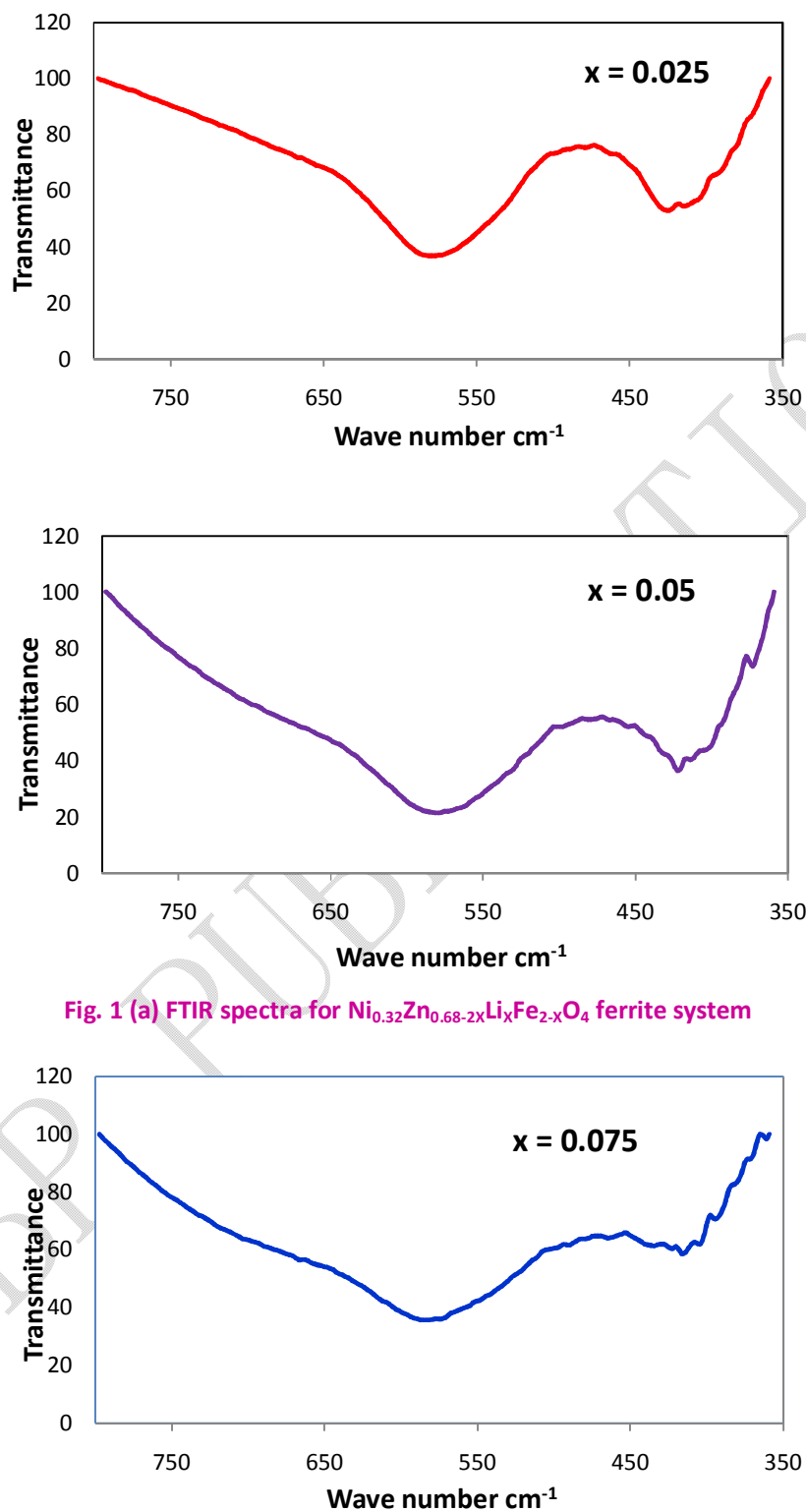


Fig. 1 (a) FTIR spectra for  $\text{Ni}_{0.32}\text{Zn}_{0.68-2x}\text{Li}_x\text{Fe}_{2-x}\text{O}_4$  ferrite system

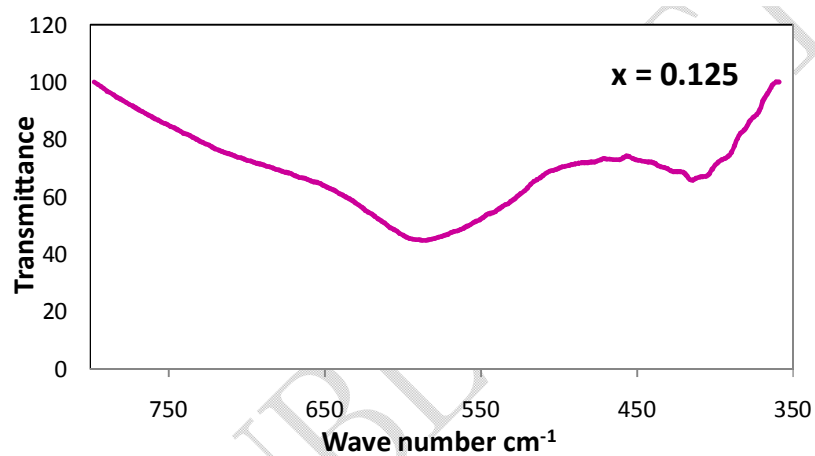
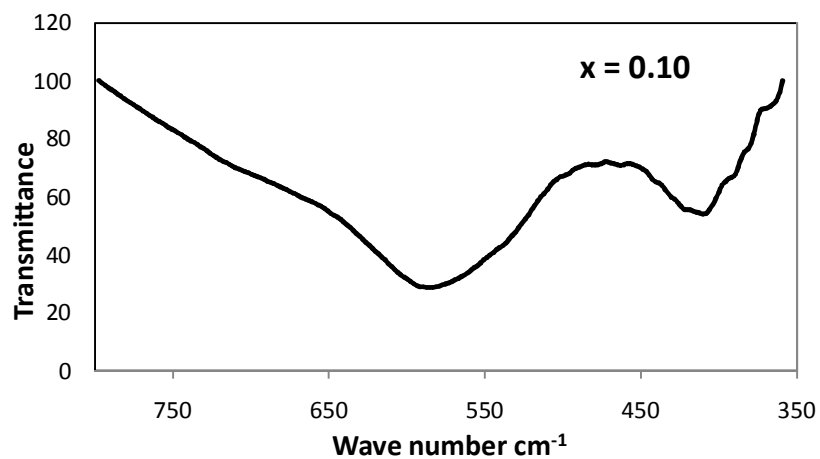
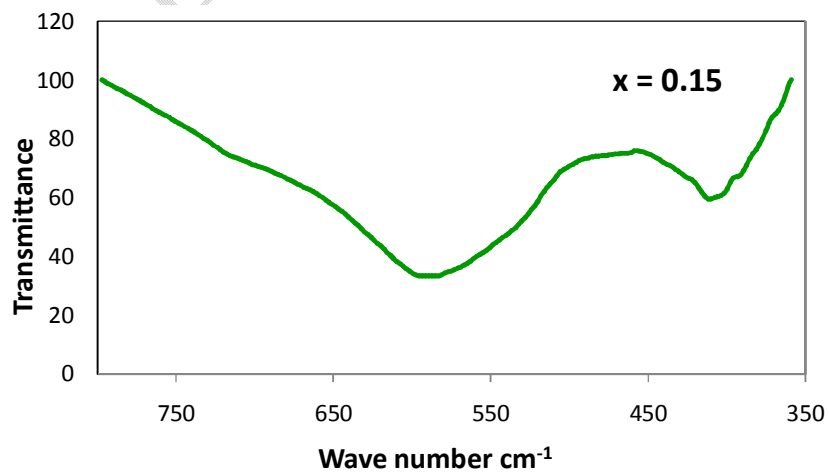


Fig. 1 (b) FTIR spectra for  $\text{Ni}_{0.32}\text{Zn}_{0.68-2x}\text{Li}_x\text{Fe}_{2-x}\text{O}_4$  ferrite system



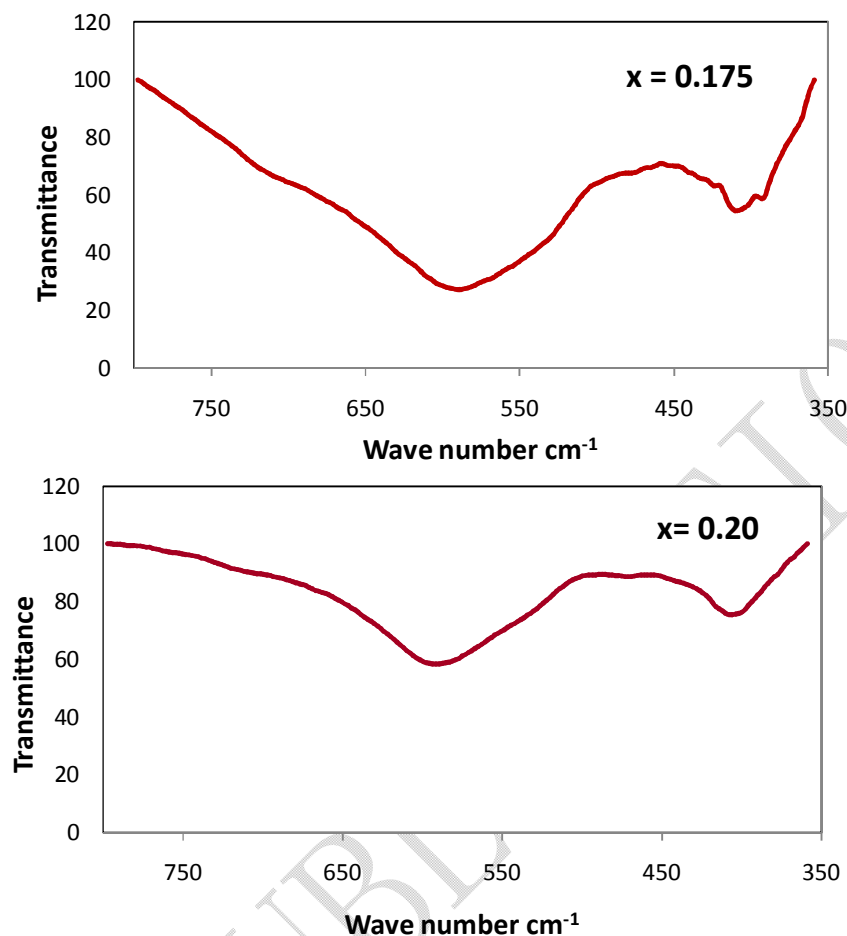


Fig. 1 (c) FTIR spectra for  $\text{Ni}_{0.32}\text{Zn}_{0.68-2x}\text{Li}_x\text{Fe}_{2-x}\text{O}_4$  ferrite system

The force constants corresponding to tetrahedral and octahedral site were calculated using the method suggested by Waldron. The force constants in terms of molecular weight of cations on A and B site and absorption band position are determined using the relation given by Pathak et al [25],

$$K_1 = 7.62 \times M_1 \times v_1^2 \times 10^{-7} \text{ N/m}$$

$$K_0 = 10.62 \times \frac{M_2}{2} \times v_2^2 \times 10^{-7} \text{ N/m}$$

Where  $K_1$  and  $K_0$  are force constants of tetrahedral and octahedral sites,  $M_1$  and  $M_2$  are the molecular weight of tetrahedral and octahedral sites obtained from the cation distribution  $[\text{Zn}_{0.68-2x}\text{Fe}_{0.32+2x}]^A (\text{Ni}_{0.32}\text{Li}_x\text{Fe}_{1.68-x})^B \text{O}_4^{2-}$ ,  $v_1$  and  $v_2$  are the corresponding centre frequency on tetrahedral and octahedral sites.

**Table 1: Data on vibrational bands ( $\nu_1$  and  $\nu_2$ ), force constants ( $K_t$  and  $K_0$ ) and longitudinal modulus (L), shear modulus (G), Bulk modulus (B), Young modulus (E) for present ferrite system.**

X	$\nu_1$ cm <sup>-1</sup>	$\nu_2$ cm <sup>-1</sup>	$K_t$ (N/m)	$K_0$ (N/m)	L (GPa)	G (GPa)	B (GPa)	E (GPa)
0.00	579	424	159.22	107.49	159.04	53.0134	88.3557	132.53
0.025	579	426	158	107.6	158.416	52.8054	88.0091	132.01
0.05	580	422	157.33	104.17	155.985	51.9948	86.6581	129.99
0.075	585	416	158.81	100.1	154.481	51.4937	85.8228	128.73
0.10	585	410	158.35	96.144	151.899	50.6329	84.3882	126.59
0.125	586	415	156.86	97.385	151.804	50.6013	84.3356	126.50
0.150	586	410	155.61	93.961	149.068	49.6895	82.8158	124.23
0.175	588	409	155.42	92.417	148.067	49.3556	82.2593	123.39
0.20	591	407	155.74	90.44	147.148	49.0493	81.7488	122.62

The variations of force constant  $K_t$  and  $K_0$  with increase in Li<sup>1+</sup> content are shown in Table 1. It is observed that both the force constant  $K_t$  and  $K_0$  decreases with increasing Li<sup>1+</sup> in Ni-Zn ferrites.

Debye temperature for present ferrite composition was determined using equation given by [22, 26] and tabulated in Table 3.

$$\theta_1 = \lambda c v_{av} = 1.438 v_{av}$$

Where  $v_{av} = \left( \frac{\nu_1 + \nu_2}{2} \right)$

It is observed that Debye temperature decreases with increasing Li<sup>1+</sup> substitution and found between 715 to 722 K. Mazen S. A. et al [27] have observed that a decrease in Debye temperature with increase in Mn content in Li-Mn ferrites and discussed this behaviour is on the basis of specific heat theory in which the electrons absorbed the part of heat hence  $\theta_1$  decreases suggesting the conduction process is mainly due to electrons.

The longitudinal  $V_L$  and transverse  $V_T$  wave velocity were calculated using the relation [28],

$$V_L = \left( \frac{C_{111}}{\rho_a} \right)^{1/2} \quad V_t = \frac{V_L}{\sqrt{3}}$$

The average force constant  $k$  is the product of stiffness constant ( $C_{111} = L$ , longitudinal modulus and lattice constant ( $a$ ).  $\rho_a$  is the density. Both the values of longitudinal and transverse wave velocities are observed to decrease with increase in Li<sup>1+</sup> content. It is also observed that the values of transverse wave velocity are less than the longitudinal wave velocity. This behaviour is explained by Lakani et al [29] as in case of transverse wave velocity, the particles in the medium vibrate perpendicular to the direction of propagation of wave motion, hence it required larger energy to make the neighbouring particles vibrate accordingly resulting in the reduction in the energy of wave and hence the velocity of transverse wave is nearly half of the velocity of longitudinal wave.

The elastic moduli, Poisson's ratio and mean wave velocity was determined using the following relation [30].

$$\begin{aligned} \text{Shear Modulus (G)} &= \rho \times (V_t)^2 \\ \text{Bulk modulus (B)} &= L - \left( \frac{4}{3} \right) G \\ \text{Young's Modulus (E)} &= (1 + \sigma) 2G \end{aligned}$$

$$\text{Poisson's ratio } (\sigma) = \frac{3B - 2G}{6B + 2G}$$

$$\text{Mean wave velocity } (V_m) = \left[ \frac{1}{3} \left( \frac{1}{V_L^3} + \frac{2}{V_t^3} \right) \right]^{-1/3}$$

Using the value of mean wave velocity Debye temperature  $\theta_D$  was determined using the Anderson's relation [31].

$$\text{Debye temperature } (\theta_D) = \frac{h}{K_B} \left( \frac{3\rho q N_A}{4\pi M} \right)^{1/3} V_m$$

Where  $h$  = Planck's constant,  $K_B$  = Boltzmann constant,  $N_A$  = Avogadro's number,  $M$  = Molecular weight of the composition,  $q$  = Number of atoms in unit formula,  $\rho$  = density of the sample

The values of these elastic moduli are tabulated in Table 1 and 2. It is observed that all these elastic moduli decreases with increase in  $\text{Li}^{1+}$  content. That may be due to inter atomic bonding between various atoms which getting weakened continuously. Similar observations have been made by Patilet. al [32] for Co-Zn ferrites.

The Debye temperature  $\theta_D$  obtained from Anderson formula are given in Table 3. It is observed that Debye temperature obtained from Waldron equation is higher than that of Anderson formula. It is also observed that  $\theta_D$  decreases with increase in  $\text{Li}^{1+}$  content as similar to the Debye temperature  $\theta_1$  obtained from Waldron's equations. Debye temperature represents the temperature at which all the modes of vibrations are excited and decrease in it implies the decrease in rigidity of ferrite materials.

As the polycrystalline ferrite materials are porous then the values of elastic constants have been corrected to zero porosity. The elastic moduli corrected to zero porosity are determined using Hasselman and Fulrath formulae [33].

$$\frac{1}{E_0} = \frac{1}{E} \left[ 1 - \frac{3f(1-\sigma)(9+5\sigma)}{2(7-5\sigma)} \right]$$

$$\sigma_0 = \left[ \frac{E_0}{2G_0} - 1 \right]$$

$$\frac{1}{G_0} = \frac{1}{G} \left[ 1 - \frac{15f(1-\sigma)}{(7-5\sigma)} \right]$$

$$L_0 = K_0 + \frac{4}{3}G_0$$

$$K_0 = \left[ \frac{E_0 G_0}{3(3G_0 - E_0)} \right]$$

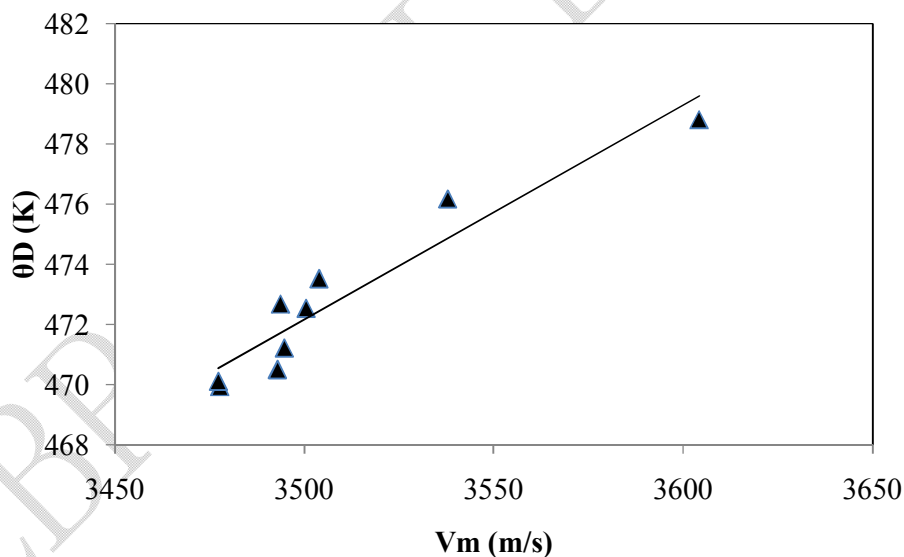
The elastic moduli corrected to zero porosity are given in Table 2. It is observed that the magnitudes of elastic constants corrected to zero porosity are higher than that of elastic constants which are not corrected to zero porosity.

**Table 2: Data on longitudinal wave velocity ( $V_L$ ) and Transverse wave velocity ( $V_T$ ), Mean wave velocity ( $V_M$ ), Poissons ratio ( $\sigma$ ), elastic moduli corrected to zero porosity ( $E_0, G_0, B_0, L_0, \sigma_0$ )**

X	$V_L$ (m/s)	$V_T$ (m/s)	$V_M$ (m/s)	$E_0$ (GPa)	$G_0$ (GPa)	$B_0$ (GPa)	$L_0$ (GPa)	$\sigma$	$\sigma_0$
0.00	5623	3246	3604	152.66	60.84	103.70	184.82	0.25	0.254
0.025	5519	3187	3538	139.82	55.85	93.90	168.36	0.25	0.251
0.05	5466	3456	3504	134.72	53.84	90.21	161.99	0.25	0.251
0.075	5450	3146	3454	132.66	53.03	88.77	159.48	0.25	0.250
0.10	5452	3148	3495	133.47	53.32	89.58	160.66	0.25	0.251
0.125	5461	3153	3500	132.73	53.03	89.02	159.73	0.25	0.251
0.150	5449	3146	3493	132.32	52.85	88.92	159.38	0.25	0.251
0.175	5425	3132	3478	129.18	51.62	86.62	155.43	0.25	0.251
0.20	5425	3132	3478	128.31	51.27	86.02	154.38	0.25	0.251

Fig. 2 shows the plot of mean sound velocity  $V_m$  against the Debye temperature obtained from Anderson formula. It is observed that mean sound velocity increases linearly with the Debye temperature indicating the direct relationship between acoustic parameter and thermodynamic parameter i.e mean sound velocity and Debye temperature. Similar relationship is observed by Reddy et al [34] for Mn-Mg ferrites and Ravinder et al [35] for Li-Mn ferrites.

The phonon frequency for each composition was determined from FTIR spectra and tabulated in Table 3. It is observed that the value of  $\nu_{ph}$  at A site is slightly larger than that of  $\nu_{ph}$  at B site. This may be due to A site is characterized by the covalent bond only and B site by both ionic and covalent bond. S. A. Mazen et al [36] have been observed similar observation for Li-Mn ferrites.

**Fig. 2 Plot for Debye temperature  $\theta_D$  against mean sound velocity  $V_m$ .**

The ratio of Bulk modulus to Rigidity modulus represents the ductility/brittleness nature of synthesized material – this is the Pugh criteria [37]. If this ratio is larger than the critical value 1.75 the material is said to be ductile in nature and if lower than 1.75 then the brittle nature. For the present ferrite system the ratio is presented in Table 3 and the values are found to be in the range of 1.68 -- 1.70 i.e slightly smaller than the critical value. Hence the synthesized ferrite materials are found to be of brittle in nature.



**Table 3: Data on Debye temperatures ( $\theta_D$ ,  $\theta_1$ ),  $B_0/G_0$  ratio, Phonon frequency [ $v_{ph}$  (A site) and  $v_{ph}$  (B site)]**

X	$\theta_D$ (K)	$\theta_1$ (K)	$B_0/G_0$	$v_{ph}$ (A site) Hz	$v_{ph}$ (B site) Hz
0.00	478.80	721.16	1.70	$1.735 \times 10^{13}$	$1.271 \times 10^{13}$
0.025	476.17	722.60	1.68	$1.735 \times 10^{13}$	$1.277 \times 10^{13}$
0.05	473.52	720.44	1.67	$1.738 \times 10^{13}$	$1.265 \times 10^{13}$
0.075	472.67	719.72	1.67	$1.753 \times 10^{13}$	$1.247 \times 10^{13}$
0.10	471.21	715.40	1.68	$1.753 \times 10^{13}$	$1.229 \times 10^{13}$
0.125	472.53	719.72	1.68	$1.756 \times 10^{13}$	$1.244 \times 10^{13}$
0.150	470.50	716.12	1.68	$1.756 \times 10^{13}$	$1.229 \times 10^{13}$
0.175	469.92	716.84	1.68	$1.762 \times 10^{13}$	$1.226 \times 10^{13}$
0.20	470.11	717.56	1.68	$1.771 \times 10^{13}$	$1.22 \times 10^{13}$

**CONCLUSIONS:**

- 1] Various compositions of Li<sup>1+</sup> substituted Ni-Zn ferrites were synthesized using oxalate precursor method.
- 2] Formation of spinel structure was confirmed using FTIR spectra which designate two absorption bands one for tetrahedral site (579-591 cm<sup>-1</sup>) and other for octahedral site (407-424 cm<sup>-1</sup>). Tetrahedral absorption bands increases with increase in Li<sup>1+</sup> whereas octahedral band decreases.
- 3] The force constants for two sites were calculated and found that both force constants decreases with increasing Li<sup>1+</sup> content.
- 4] The wave velocity, elastic constants and Debye temperature were determined using FTIR data and found to decrease with increasing Li<sup>1+</sup> content in Ni-Zn ferrites.
- 5] Elastic moduli are corrected to the zero porosity.
- 6] The bulk modulus to rigidity modulus ratio indicates the brittle nature of synthesized materials.

**REFERENCE:**

- 1] M. Sertkal, Y. Koseoghi, A. Baykal, H. Kavas, A. Bozkurt, M. S. Toprak: J. Alloys & Comp., 486 (2009) 325
- 2] S. E. Shirsath, S. S. Jadhav, B. G. Tiksha, S. M. Patange, K. M. Jadhav: Scripta Mater., 64 (2011) 773
- 3] A. Goldman: "Modern Ferrite Technology", Van Nostrend Reinhold, NY, 1990
- 4] X. Y. Zhang, J. Xu, Z. Z. Li, W. H. Qi, G. D. Tang, Z. F. Shang, D. H. Ji, L. L. Lang: Physica B, 446 (2014) 92-99
- 5] M. Srivastava, A. K. Ojhab, S. Chaubeya, P. K. Sharma, A. C. Pandey: Mater. Sci. Eng. B., 175 (2010) 14-21
- 6] P. A. Jadhav, R. S. Devan, Y. D. Kolekar, B. K. Chaugule: J. Phys. & Chem. Solids, 70 (2009) 396-400
- 7] M. Fedar, L. Diamandescu, I. Bibicu, O. F. Caltun, I. Dimitru, L. Boutiuc, H. Chiriac, N. Lupu, V. Vilceanu, M. Vilceanu: IEEE Trans. Magn., 44 (2008) 2936
- 8] M. R. Barati, S. A. S. Ebrahimi, R. Dehghan: IEEE Trans. Magn., 45 (2009) 2561
- 9] S. H. Yu, T. Fujino, M. Yoshimura: J. Magn. Magn.Mater., 256 (2003) 420
- 10] I. H. Gul, W. Ahmed, A. Maqsood: J. Magn. Magn.Mater., 320 (2008) 270
- 11] C. W. Fu, M. R. Syue, F. J. Wei, C. W. Cheng, C. S. Chou: J. Appl. Phys., 107 (2010) 09A519
- 12] N. Rezlescu, E. Rezlescu, C. Pasnicu, M. L. Craus: J. Phys. Conden. Matter, 6 (1994) 5707
- 13] N. Rezlescu, E. Rezlescu, C. Pasnicu, M. L. Craus: Magn. Magn.Mater., 136 (1994) 319
- 14] N. Rezlescu, E. Rezlescu: Solid state Comm., 88 (1993) 139
- 15] G. S. Shahane, K. Ashok, A. Manju, P. P. Pant, L. Krishan : J. Magn. Magn.Mater., 322 (2010) 1015
- 16] Sihan Lin, Yusheng He, Chongde Wei, ZhaahulShen: Supercond. Sci. Tech., 2 (1989) 145
- 17] V. K. Lakani, K. B. Modi: Solid State Sci., 12 (2010) 2134
- 18] P. Venugopal Reddy, T. SheshagiriRao: Solid State Comm., 56 (1985) 985
- 19] D.G.Wickham, in S.Young Tyree, Jr. (Ed): "Inorganic Synthesis", 9, II nd edition, McGraw Hill Book Com., NY (1967) 152
- 20] M.Bremer, St.Fisher, H.Langbein, W.Topelmann, H.Scheler: Thermo. Acta., 209 (1992)323
- 21] D. Dollimore, D. Tinsley: J. Chem. Soc., A, (1971) 3043-47

- 22] R. D. Waldron: Phys. Rev., 99(06), (1955) 1727-35
- 23] A. E. Lavat, E. J. Baran: J. Alloys & Comp., 368 (2004) 130
- 24] A. E. Lavat, E. J. Baran: J. Alloys & Comp., 419 (2006) 334
- 25] T. K. Pathak, J.J.U. buch, U.N.Trivedi, H.H.Joshi, K.B.Modi: J. Nanosci. & Nanotech., 8 (2008) 4181-4187
- 26] S. A. Mazen, H. M. Zaki, S. F. Mansour: Inter. J. Pure & Appl. Phys., 3(1), (2007) 40-48
- 27] S. A. Mazen, N. I. Abu-Elsaad: ISRN Cond. Matt. Phys., Vol. 2012, Article ID 907257, 9 Pages.
- 28] W.A.Wooster: Rep. Prog. Phys., 19 (1953) 62
- 29] V.K.Lakhani, K.B.Modi: Solid State Sci., 12 (2010) 2134
- 30] V.Baldev Raj, P.Rajendran, Palanichamy: "Science and Technology of Ultrasonics", Narosa Pub. House, New Delhi, (2004), 250
- 31] O.L.Anderson: "Physical Acoustics", Vol. III, Part B, Academic Press, NY, USA, (1965), 43
- 32] V.G.Patil, S.E.Shirsath, S.D.More, S.J.Sukla, K.M.Jadhav: J.Alloys and Compounds, 488, (2009), 199-203
- 33] D.P.N. Hasselmann, R.M. Fulrath: J. Am. Ceram. Soc., 47, (1964), 52-53
- 34] P. V. Reddy: Phys. Stat. Sol. A, 108(2), (1988) 607-611
- 35] D. Ravinder, L. Balachander, Y. C. Yenudhar: Mater. Lett., 49(3-4) (2001) 205-208
- 36] S.A.Mazen, N.I. Abu Elsaad: ISRN Cond. Matter Phys., (2012), Article ID 907257, 1-9
- 37] S.F.Pugh: Phil. Mag., 45, (1954), 823-843